Transportation Research Part C 44 (2014) 21–33

Contents lists available at ScienceDirect

Transportation Research Part C

journal homepage: www.elsevier.com/locate/trc

Microscopic modeling of pedestrian movement behavior: Interacting with visual attractors in the environment

W.L. Wang [a], S.M. Lo [a,*], S.B. Liu [b], H. Kuang [a]

[a] Department of Civil and Architectural Engineering, City University of Hong Kong, Tat Chee Avenue, Kowloon, Hong Kong
[b] Department of Systems Engineering and Engineering Management, City University of Hong Kong, Tat Chee Avenue, Kowloon, Hong Kong

ARTICLE INFO

Article history:
Received 9 March 2014
Received in revised form 12 March 2014
Accepted 12 March 2014

Keywords:
Pedestrian movement behavior
Microscopic modeling
Visual attractors
Impulse stops

ABSTRACT

Goal-directed pedestrian movement behavior is extensively studied by researchers from varied fields, but pedestrian's movement actions such as 'impulse stops' resulting from exploratory movement behavior receive little attention. To understand this, an effective tool that can reveal the attractive interactions between pedestrians and attractors in the environment is needed. This study introduces an agent-based microscopic pedestrian simulation model—CityFlow-U. To determine whether a pedestrian would stop for visual attractors, factors of attractor's attractiveness, distance to the attractor as well as the visibility of the attractor from current location of the agent are considered. By analyzing the parameters in this model, we have successfully revealed different pedestrian movement modes, attractor preferences and movement trajectories in a notional setting. The reliability of the model is then demonstrated with a simulation scenario targeting at a circulation region of a shopping mall in Hong Kong. Observational data is used for model input and the number changes of attracted pedestrians in front of a major attractor are compared between simulation results and empirical video data. Results from the parameter analysis and simulation scenario show that the model is flexible and can benefit in real applications such as shop arrangement as well as street furniture placement.

1. Introduction

Pedestrian dynamics has received increasing attention from various fields including building evacuation (Lo et al., 2004; Shiwakoti and Sarvi, 2013; Zheng et al., 2009), transportation engineering (Davidich et al., 2013; Yuen et al., 2013; Zeng et al., 2014), physics (Helbing and Molnár, 1995), urban design (Yin, 2013), and marketing (Dijkstra et al., 2011). In order to understand collective pedestrian movement patterns through space, different microscopic simulation models have been developed such as Cellular Automaton model (Bandini et al., 2007, 2014; Burstedde et al., 2001), social force model (Helbing and Molnár, 1995; Kwak et al., 2013; Song and Duh, 2010) and agent-based model (Bandini et al., 2011; Dijkstra, 2008; Ma et al., 2013; Schelhorn et al., 1999). With these models, many pedestrian flow phenomena such as lane formation (Hua et al., 2010; Ma et al., 2010), crowd passing through a bottleneck (Dai et al., 2013), and intersecting pedestrian flows (Guo et al., 2010) can be demonstrated. Such self-organized movement patterns of pedestrians could be reproduced to some extent by considering mainly self-driven forces to destinations and repulsive interactions with environment boundaries and other pedestrians. However, pedestrians will visually perceive and response to the environment information (especially

* Corresponding author. Tel.: +852 34427683.
E-mail address: bcsmli@cityu.edu.hk (S.M. Lo).

http://dx.doi.org/10.1016/j.trc.2014.03.009

attractive objects) in the course of moving along a path (Zacharias, 1997, 2001). In other words, visual perception and attractive interactions with the environmental stimuli are two important issues affecting pedestrian movement behaviors.

In terms of the visual information, it has been directly linked to pedestrian movement model in previous literatures. One common way is the static representation of what pedestrians can see and where they can go within space, such as Visibility Graph Analysis (VGA) (Turner et al., 2001). Turner and Penn (2002) developed an agent simulation to implement pedestrian movement with the aid of an 'exosomatic visual architecture'. But the model experienced obvious limitations in certain environment such as a long thin corridor and large open space, as pedestrian's movement decision greatly depends on the availability of a destination and configurational clues (exit). Another dynamic representation of visual information is the individual fan-shaped vision field (Asano et al., 2010; Moussaïd et al., 2011; Park et al., 2013), which can help implement natural movement of pedestrians. It is usually discretized into limited number of choice sets (directions) to reduce computing costs, and then pedestrian's desired walking direction and desired walking speed is determined by certain rules or mechanisms. However, all these previous models only take the selected goal as the pedestrian's main drive, and all the other objects in the environment, no matter how attractive they are, would be regarded as obstacles.

Pedestrian perceives the environment as they walk, during which they may be influenced by visual attractors such as window displays or street performances. If the object is attractive enough and meets the pedestrians' demands, they would even stop walking and visit it, namely 'impulse stops' (Borgers and Timmermans, 1986; Cobb and Hoyer, 1986). Though it is of great influence on movement behavior, the attractive interactions between pedestrians and visual attractors in the environment received little attention in previous literatures. The STREETS model (Schelhorn et al., 1999) incorporated the concept of 'fixation' to represent the pedestrian behavior that being distracted from their plans, but the mechanisms seemed too random. Chen (2011) introduced the 'attention theory' to pedestrian behavioral model and used an actual street case to simulate the pedestrian movements in urban spaces. However, how pedestrians perceive and interact with environmental attractors in the model was not clear. In a recently published paper, Kwak et al. (2013) extended the social force model by incorporating the attractive interactions between pedestrians and attractions and presented a phase diagram with various collective patterns of pedestrian movements. But it is not practical that only homogeneous properties of pedestrians and attractions were considered in the model.

Although extensive studies have been performed to simulate pedestrian dynamics, limited research works are available in the literatures examining the interactions between pedestrians and environmental attractors based on pedestrian's visual perception. This has motivated our research, the goal of which is to develop a microscopic simulation model that can reveal the realistic pedestrian movement behaviors and explain its mechanism. CityFlow-U is an expanded version of CityFlow which has recently been developed by City University of Hong Kong (Liu et al., in press). A new module named *attention-based exploratory movement module* has been added and analyses on critical parameters have also been provided. This module enables the agent to explore the visual attractors and then decide whether it will be distracted from the pre-defined routes by examining attractor characteristics and agent's internal state of demand. To demonstrate the reliability of the module, a simulation scenario about a circulation region of a shopping mall was presented. Observational data was used for model input and the number changes of attracted pedestrians in front of a major attractor were compared between simulation results and empirical video data. Finally, we drew some conclusions and proposed future researches.

2. Simulation model: CityFlow-U

2.1. Overview of CityFlow-U

The original model was implemented by two modules at three levels: (1) the *route choice and map navigation module* identifies the temporary desired regional target of movement, reflecting strategic, tactical level behavior in macroscopic scope; (2) the *agent-based individual movement module* decides the local movement of the agents based on detailed environmental information at every time step, reflecting operational level behavior in microscopic scope. When the regional target is reached, the second module will convey the message back to the first module and request for the next one until final goal is approached. In CityFlow-U, a new module namely (3) the *attention-based exploratory movement module* has been added which examines characteristics of the external attractors and agent's internal state of demand at operational level in microscopic scope. Once the attractor meets the agent's requirement, the message on changing the regional target will be sent back to the first module, as shown in Fig. 1.

Besides information about the environment, the properties of the agents to be simulated and the demand of the pedestrian system are required as inputs for the model, visual attractor characteristics are new essential data for representing external stimuli in the environment. Specifically, spatial layout of the visual attractor, its type and attractiveness need to be prepared. The building space in the simulation is represented in a network approach by dividing the geometry into 'zones' (including regular space and visual attractors) connected to one another by 'connections'. Fig. 2 shows an example of the space representation. Each zone is defined in a 2D continuous space by lines specifying the geometry boundaries. Zones in the space geometry are connected by 'arcs' which are actually virtual links between zones representing the features of routes, including distance, type and capacity of a route. As some pedestrians may change their plans by visiting visual attractors, these routes are connected by 'dashed arcs'.

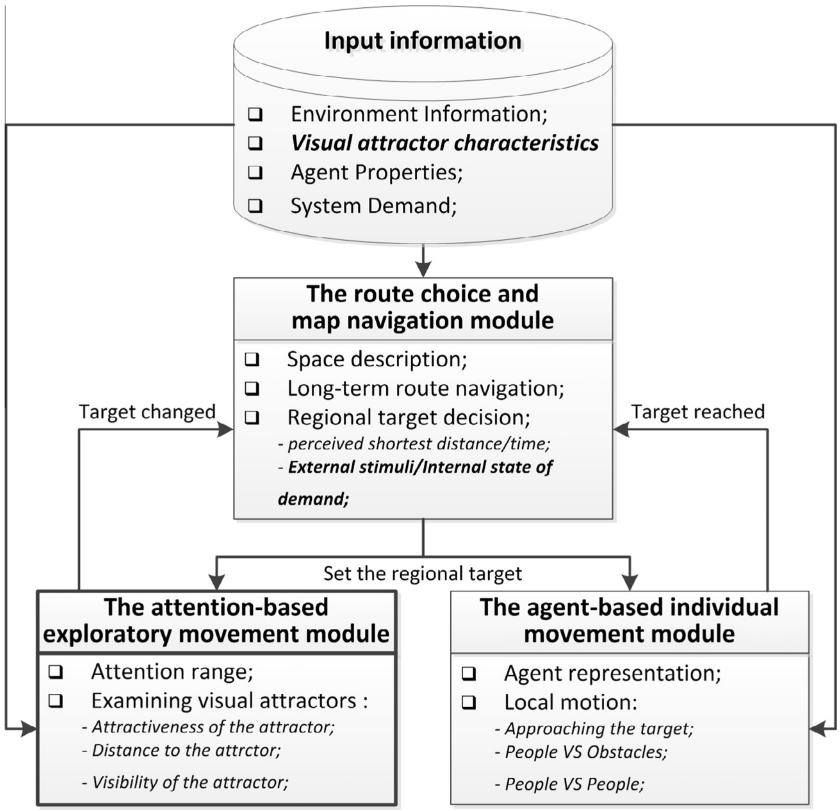

Fig. 1. Framework of CityFlow-U.

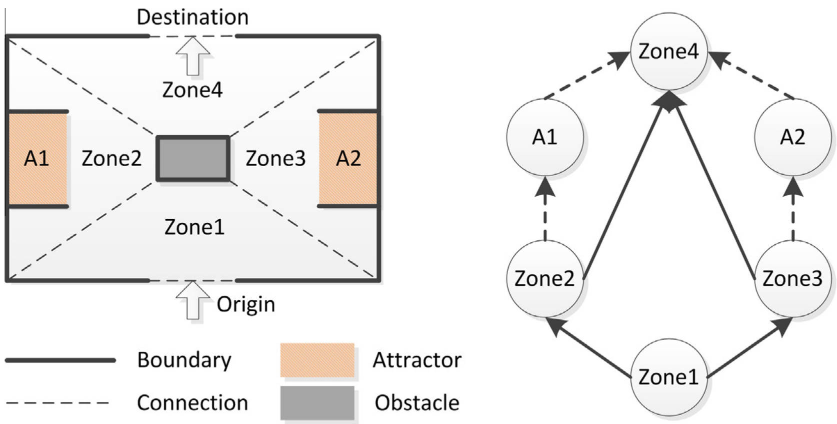

Fig. 2. Space representation.

In terms of local movement at microscope level, the *agent-based individual movement module* treats every pedestrian as an agent in the shape of a circle with a view range. The diameter of the circle is set to be 0.4 m in the model, which is the typical body size of a person. The view angle is set as 170°, and discretized into subangles to reduce the computational burden without losing accuracy. The depth of the view range is set to 3 m in the model, and only the area within the view range is considered effective for the pedestrian to make a decision for movement. Agents move one step per time step toward the direction calculated by a utility maximization approach in which various factors that influence pedestrian's movement are considered, including the efficiency of approaching the target point, the interaction between pedestrians and obstacles, the interaction between pedestrians, and inertia of pedestrians. Once a direction is chosen, the agent can move forward one step with proper movement speed, which considers both the available movement distance, density of the view range as well as the desired speed of the agent.

2.2. pedestrian visual attention and behavior analysis

When walking in complex built environment, pedestrians' actions are governed by both goal-directed and exploratory behaviors (Gibson, 1988). Goal-directed behavior typically refers to the motivation of moving to certain points in space such as residential buildings and transit terminals. Exploratory behavior is usually stimulated by visually attractive objects along the path to the goal, for instance, window displays and street performance. And the ability to perceive and interact with the visual attractors in the built environment is defined as 'visual attention' in this study. Specifically, it would influence the pedestrians' spatial selection based on the results of examining the internal state of demands (e.g. need to buy specific stuff) and the external stimuli (e.g. specific type of shops) in the environment.

In terms of the goal-directed behavior, the pedestrian usually performs *normal walking* towards his goals. Regarding actions to visual attractors in the environment, the pedestrian's exploratory behavior may have four stages: (1) *wandering*, walk along the scheduled path to final goal when they cannot perceive any attractors; (2) *evaluating attractors*, examine the attractiveness of external stimuli and further choose the most attractive one based on internal state of demands; (3) *being attracted*, change temporary target to the matching attractor; (4) *visiting attractors*, stop at the attractor for a few time, as shown in Fig. 3.

In our model, two types of agents are defined: normal agents and susceptible agents, as shown in Table 1. For normal agents, they would not response to the environmental stimuli and just move along the well-defined path to the goal, such as commuters who use the street as a path. As a result, they only do normal walking in the environment. In terms of sus-

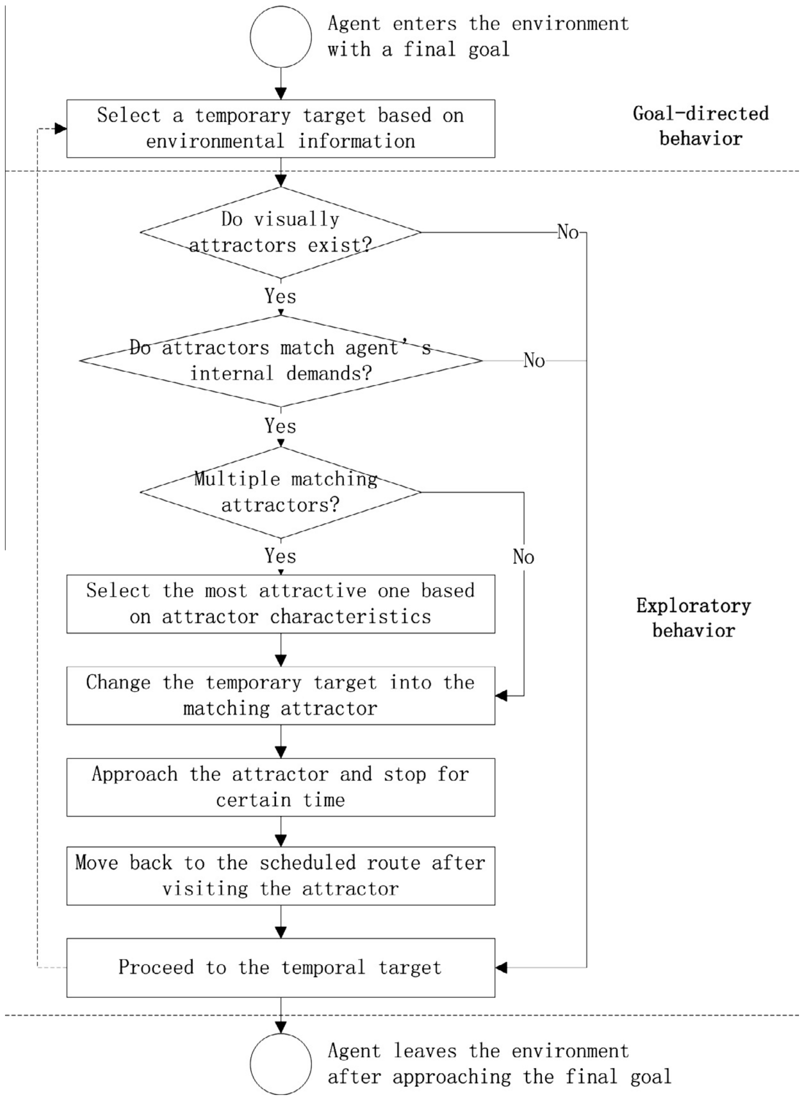

Fig. 3. Flow chart of pedestrian's movement process in the environment.

Table 1
Rules of examining external stimuli and agent's internal state of demand.

Agent type	External stimuli	Internal state (before)	Matching conditions	Internal state (after)	Movement Behavior
Normal agent	/	/	/	/	Normal walking
Susceptible agent	None	All[a]	/	All[a]	Wandering
	Object type (OT_j) and attractiveness (OA_j)	No specific type but of certain demand level (DL_i)	$T_{i,j} > DL_i$	No specific type, demand level increases	Being attracted and visiting attractors
	Object type (OT_j) and attractiveness (OA_j)	Specific demand type (DT_i and certain level (DL_i)	$DT_i \neq OT$	Demand type and level unchanged	Wandering
	Object type (OT_j) and attractiveness (OA_j)[b]	Specific demand type (DT_i) and certain level (DL_i)	$DT_i = OT$ and $T_{i,j} > DL_i$	Demand type unchanged, demand level increases	Being attracted and visiting the attractor

[a] It includes pedestrians with different internal state of demands.
[b] If multiple attractors match the demand, choose the one with best matching value.

ceptible agents, each of them has an internal state of demand (including type and level) and would wander and explore the environment until it is attracted by an attractor. Specifically, each attractor in the environment has certain type and attractiveness, depending on which pedestrians may have 'impulse stops'. Only when the type of an attractor matches the pedestrian's expectation and the tendency to visit the attractor (can be calculated through Eq. (1)) is greater than its demand, the pedestrian will change its plan to visit the attractor. Similarly, the pedestrian without specific demand type will be attracted as long as the tendency to visit the object is higher than its demand. Otherwise, pedestrians will continue wander and explore other interested visual attractors.

Since human's perception is limited especially in the environment with intensive visual attractors like shopping street, it is not realistic that the pedestrian responses to every attractor. An empirical study conducted by Zhuang et al. (2006) demonstrated that the number of stores visited has a negative influence on shoppers' purchase behavior. One possible reason could be that the more shops the agent visits, the higher probability its demand has been fulfilled (its demand level will correspondingly increases, and attractors with higher perception level will be chosen to visit afterward). As a result, during the movement process of a susceptible agent, its internal state of demands would be modified as a result of perception of external stimuli.

2.3. The attention-based exploratory movement module

When moving in a space, the range we can perceive is usually further than that we use for configuration of movement. For example, we may notice a distant eye-catching signboard, but do not need to avoid pedestrians far away. It is the reason that we design a unique radial and individual-based attention range to interact with the environmental stimuli. Unlike the view range in the *agent-based individual movement module*, angle of attention range (θ_a) in this module is 120° and the depth of range (R_a) is set to be 10 m (Chen, 2011). The attention range is divided into sectors originating at the individual locations. The central sector is oriented with the current direction of the pedestrian, as shown in Fig. 4.

As indicated in Table 1, normal agents will not be influenced by the attractors at all, and thus susceptible agents are our focus in this module. We firstly exam the agent's internal state of demand and external attractor characteristics to determine whether the agent's next temporary target would be changed. When the tendency value of agent i to visit attractor j ($T_{i,j}$) calculated from Eq. (1) is greater than the internal demand level of the agent (DL_i), it will choose the matching attractor j as its next temporary target. Otherwise, the agent will continue to move on the pre-defined route.

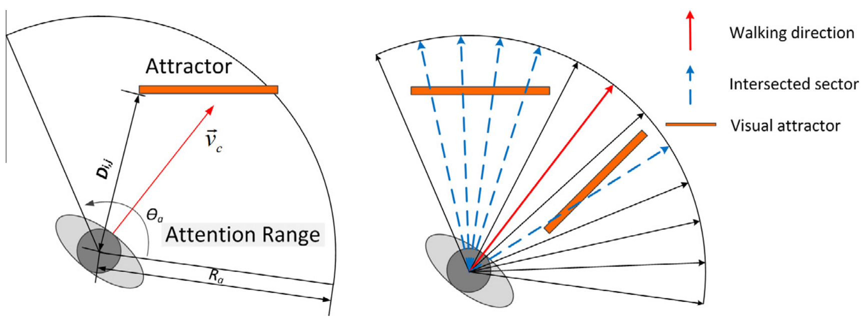

Fig. 4. Visual attention range of simulated agent.

$$T_{i,j} = \omega_m \cdot P_{i,j}$$
$$\text{where } \omega_m = \begin{cases} 1 & DT_i = OT \text{ or } DT_i = null \\ 0 & otherwise \end{cases} \quad (1)$$

Based on the perception of agent *i* on attractor *j* ($P_{i,j}$), we introduce an binary matching parameter ω_m to obtain the tendency value $T_{i,j}$. Agent who has specified demand (DT_i) will prefer to visit the attractor of same type ($DT_i = OT$, *then* $\omega_m = 1$), or it may not be so interested in ($DT_i \neq OT$, *then* $\omega_m = 0$). For the susceptible agent who does not have specific demand type ($DT_i = null$), its tendency to visit the attractor will be the same as it has perceived ($\omega_m = 1$).

$$P_{i,j} = \delta_j^a \cdot \left(\omega_d \cdot \delta_{i,j}^d + \omega_v \cdot \delta_{i,j}^v\right) + \varepsilon \quad (2)$$

where ω_d and ω_v are the weight parameters used to adjust the sensitivity of each factor. The value range is [0,1], and the sum is set to be 1. ε is a stochastic variable representing other influencing factors. As the following listed factors are determinants of a pedestrian's perception on environmental attractors in previous literatures (Nassar, 2011; Timmermans, 2009; Xi et al., 2011), we assume influences of other factors are limited. Thus value of the stochastic variable ranges between 0 and $\min\left\{\delta_j^a \cdot \left(\omega_d \cdot \delta_{i,j}^d + \omega_v \cdot \delta_{i,j}^v\right)/2, 1 - \delta_j^a \cdot \left(\omega_d \cdot \delta_{i,j}^d + \omega_v \cdot \delta_{i,j}^v\right)\right\}$. The attractiveness ratio $\left(\delta_j^a\right)$, distance ratio $\left(\delta_{i,j}^d\right)$ and view ratio $\left(\delta_{i,j}^v\right)$ will be interpreted in detail below. In order to get the normalized value, all these ratio values also range in [0,1].

(1) Attractiveness of the attractor δ_j^a.

Attractiveness of the attractor is one of the most important factors contributing to a pedestrian's decision on changing the scheduled route and visiting it. To determine its value, we need collect information on attractor's physical characteristics such as size and color, and pedestrians' impression of the attractor, which is also part of the model input.

(2) Distance to the attractor $\delta_{i,j}^d$.

When pedestrians consider changing routes for attractors, distance is another important factor, and hence ratio of shortest distance to attractor ($D_{i,j}$) to depth of attention range (R_a) is calculated. As the nearer the attractor is, the higher chance it would be visited. Thus residual value is used in Eq. (3).

$$\delta_{i,j}^d = 1 - D_{i,j}/R_a \quad (3)$$

(3) Visibility of the attractor $\delta_{i,j}^v$.

As visually attractive objects may have different visibilities due to their locations and angular dimensions from position of the pedestrian, so number of intersected sectors with the attractor *j* ($N_{i,j}$) is checked, and N_a is the total number of sectors of the pedestrian's attention range, computed as Eq. (4).

$$\delta_{i,j}^v = N_{i,j}/N_a \quad (4)$$

Accordingly, $P_{i,j}$ can also be calculated as follows:

$$P_{i,j} = \delta_j^a \cdot [\omega_d \cdot (1 - D_{i,j}/R_a) + \omega_v \cdot N_{i,j}/N_a] + \varepsilon \quad (5)$$

The attractor with the highest tendency value (T_{max}) would be chosen if there are alternative attractors in agent's attention range. To prevent revisit at the same attractor, each attractor visited by the agent would be recorded in its travel diary.

3. Parameter analysis

For illustration, we develop a notional setting which is a shopping street segment based on symmetric geometry. Twelve shops are located along the east and west sides of the street as the visual attractors, and the west and east ends are gateways where pedestrians can enter and depart, show as Fig. 5. We reveal different pedestrian movement modes, attractor preferences and movement trajectories by analyzing the parameters described before.

3.1. Pedestrian movement modes determined by internal demands and external stimuli

Pedestrians have different goals and inner states of demands when moving in the environment, and visually attractive objects can distract them from their scheduled routes toward goals. As a result, different types of pedestrian movement modes can be revealed by changing the value of ω_m, as shown in Fig. 6.

(1) Random movement. Pedestrians' trip purposes and demands are unclear, and their moving trajectories would cover scattered shops. They can change temporal targets during the trip and usually make selections and decisions upon examining the internal state of demands and external stimuli ($\omega_m = 1$ where $DT_i = null$), as shown in Fig. 6(a).

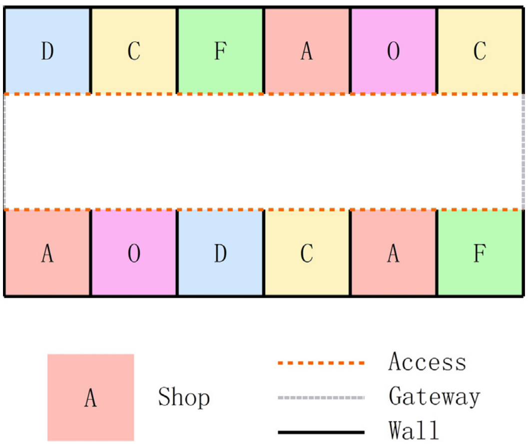

Fig. 5. Notional shopping street segment with different types of shops denoted by varied characters.

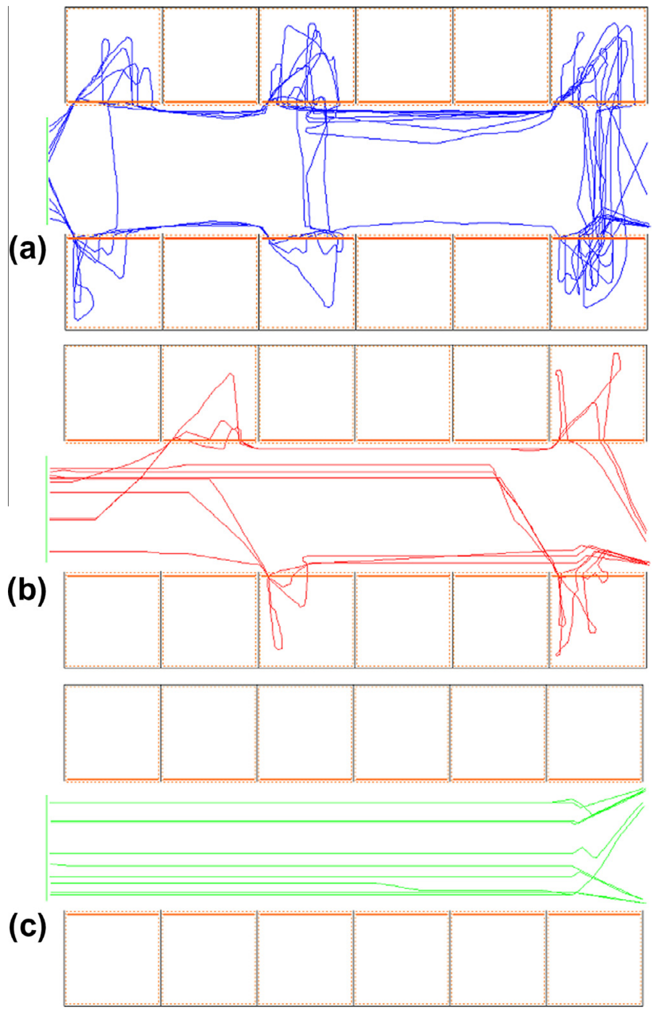

Fig. 6. Pedestrian movement modes in shopping street simulation: (a) random movement; (b) purposive movement; (c) normal movement.

(2) Purposive movement. Pedestrians' trip purposes and demands are simple and clear, so their movement trajectories are only connected by specified shops ($\omega_m = 1$ where $DT_i = OT$), as shown in Fig. 6(b).
(3) Normal movement. Pedestrians may have no demands and would not be attracted by visual attractors during the trip ($\omega_m = 0$), resulting in direct trajectories from one end of the street to the other, as shown in Fig. 6(c).

3.2. Pedestrian's perception affected by attention range depth and angle

Due to the physical limitations of attention range, pedestrians can only perceive and react to certain stimuli in the environment. As there is a lack of empirical data on pedestrian's attention range, we use four groups of dimensions for testing to find out the influences of different range depths and angles on pedestrians' perceptions of the environmental stimuli. Fifty agents with random movement behavior ($\omega_m = 1$ where $DT_i = null$) enter the street from west gateway, visit shops they are interested and would leave the street through east gateway. During the movement process, pedestrian's internal state of demand would have a certain increment (0.02) after visiting a visual attractor. Attractiveness of the shop is set to be increased from west to east, specifically, attractiveness of the westernmost two shops (δ_1^a and δ_7^a) is 0.17, the next two (δ_2^a and δ_8^a) is 0.34, and so forth, attractiveness of the easternmost two shops (δ_6^a and δ_{12}^a) is 1, as shown in Fig. 7.

Distance parameter $\omega_d = 0.5$ and visibility parameter $\omega_v = 0.5$ are used in the simulation tests. Test results are shown in Fig. 8, in which shops are rendered in different gray colors representing the corresponding patronage rates. In specific, the westernmost shops are of white color, indicating they hardly have any patronage during the simulation process. And the easternmost shops are of black color, showing that they appeal to all the pedestrians.

When searching the stimuli, pedestrians with broader attention range would include more stimuli for comparing. According to the simulation results in Fig. 8, we found that pedestrians set with diverse attention angles (comparison between Fig. 8(a) and (b) or Fig. 8(c) and (d)) do not show significant differences in shop preferences, whereas differences between

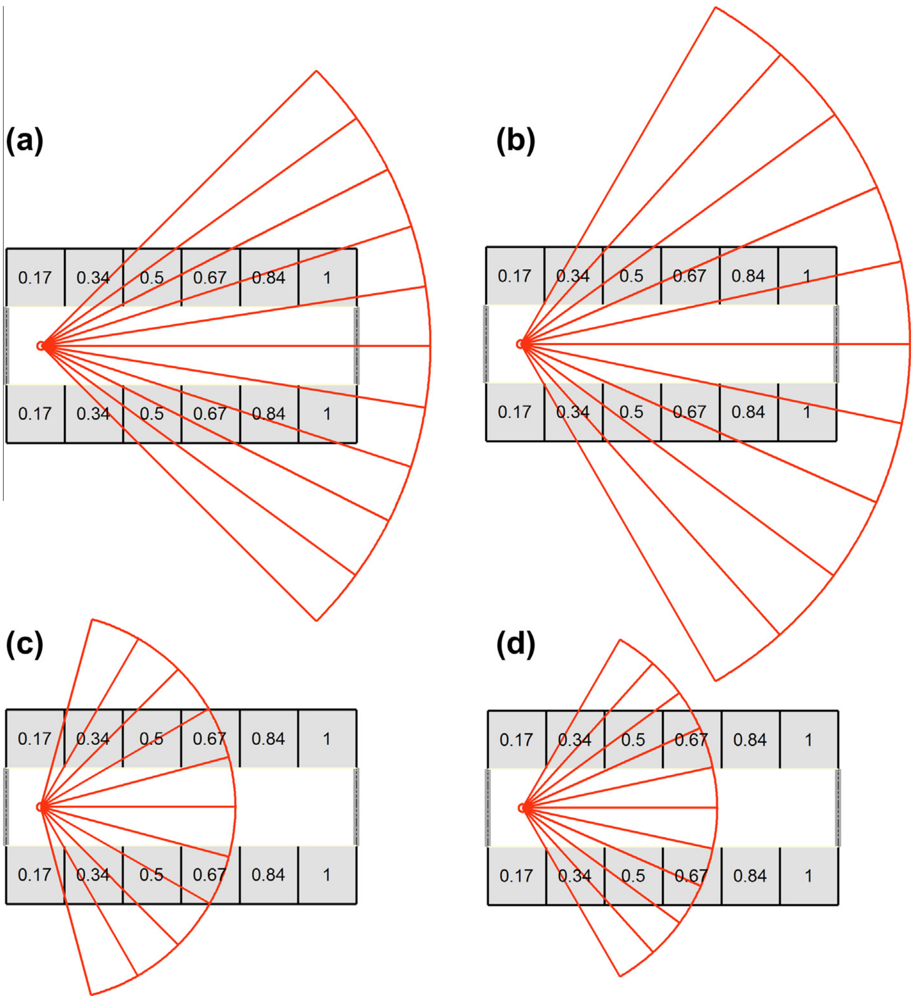

Fig. 7. Simulation test settings with different pedestrian attention depths and angles: (a) attention angle = 90°, attention depth = 20 m; (b) attention angle = 120°, attention depth = 20 m; (c) attention angle = 150°, attention depth = 10 m; (d) attention angle = 120°, attention depth = 10 m.

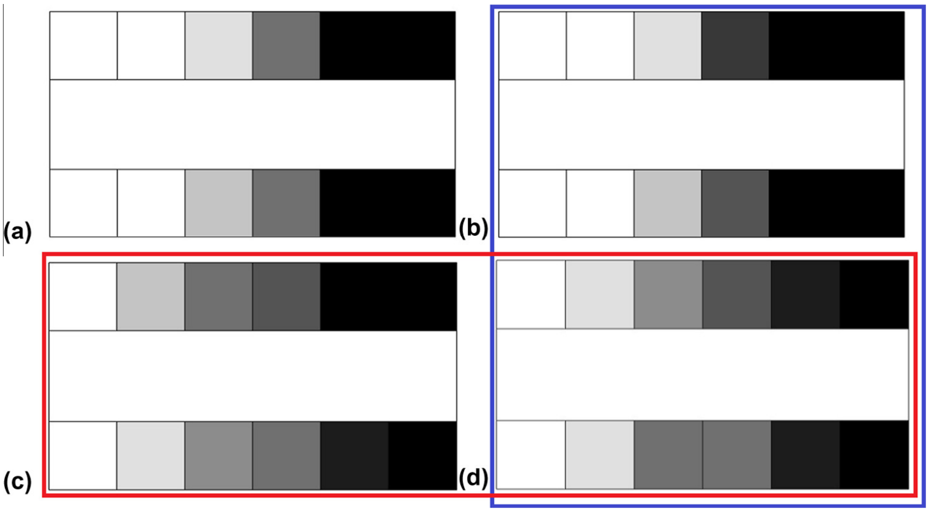

Fig. 8. Simulation results of pedestrians set with different attention depth and view angle: (a) attention angle = 90°, attention depth = 20 m; (b) attention angle = 120°, attention depth = 20 m; (c) attention angle = 150°, attention depth = 10 m; (d) attention angle = 120°, attention depth = 10 m.

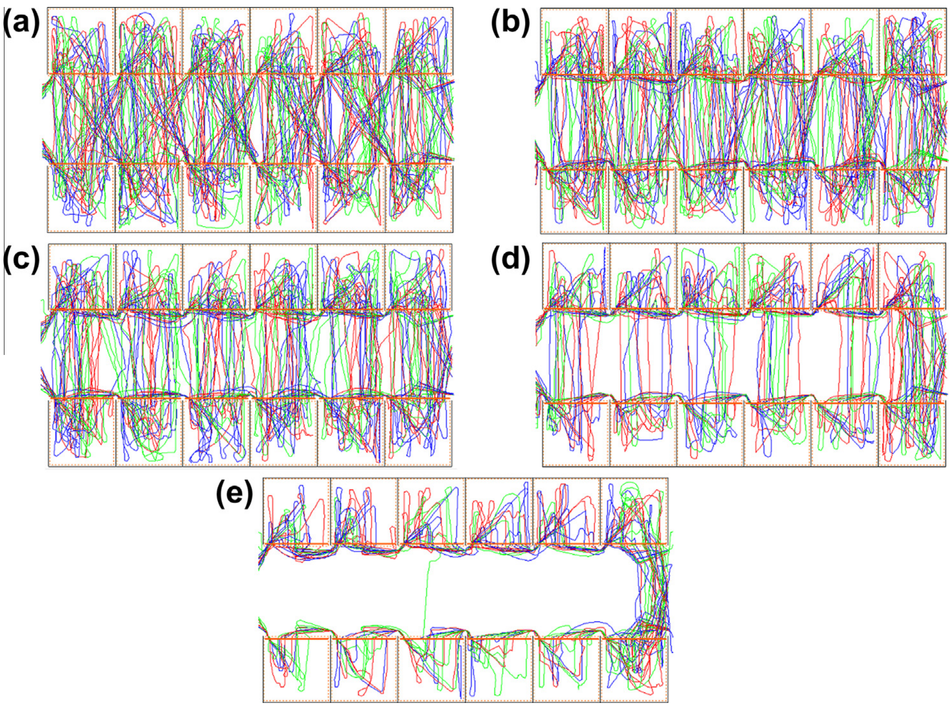

Fig. 9. Simulation results of different visibility and distance weights: (a) $\omega_v = 0.9$, $\omega_d = 0.1$; (b) $\omega_v = 0.7$, $\omega_d = 0.3$; (c) $\omega_v = 0.5$, $\omega_d = 0.5$; (d) $\omega_v = 0.3$, $\omega_d = 0.7$; (e) $\omega_v = 0.1$, $\omega_d = 0.9$.

tests of varied range depths are more obvious (Fig. 8(b) and (d)). It is possibly because external stimuli (shops) in the test settings are symmetrically allocated along the pedestrian's main route. Under these circumstances, pedestrian's attention with longer range may cover more shop alternatives especially those highly attractive ones than that with broader angle. Hence pedestrians in Fig. 8(a) and (b) tend to visit shops of higher attractiveness but located further (shops on the eastern part of the street).

3.3. Pedestrian movement trajectories influenced by visibilities of and distances to attractors

A series of tests are carried out to evaluate the sensitivity of the parameter ω_v and ω_d and identify their influences on pedestrian movement trajectories. Similar to attention range depth and angle tests in Section 3.2, fifty agents with random movement behavior ($\omega_m = 1$ where $DT_i = null$) are used. To eliminate the influences of other factors, all the shops are set to be of same attractiveness $\left(\delta_j^a = 1\right)$ and pedestrians are given very low internal demand values in the tests (0.1). The trajectory color of each agent in the Fig. 9 is randomly determined when it is generated.

We can see that an overwhelming majority of the pedestrians would like to visit shops across the street (diagonal path) in despite of longer distances in Fig. 9(a), since visibility of the shop (ω_v) dominates their shopping decisions. When pedestrians get out of a shop, they will notice the shops across the street better than those locate on the same side of the street for the limitation of its attention angle ($\theta_a = 120°$). As the value of distance parameter (ω_d) increases, some of the pedestrians prefer to visit nearby shops on the same side of the street, as shown in Fig. 9(b). And the number of pedestrians who choose to visit the shops across the street becomes very close to that of pedestrians prefer to visit nearby shops in Fig. 9(c), as the visibility of and distance to interested shops are equally important for testing pedestrians in this case. Analogously, "across" pedestrians become even less in Fig. 9(d) and almost all the trajectories of pedestrians cover only one side of the street in Fig. 9(e).

4. Simulation scenario

To demonstrate the reliability of the proposed model, a simulation case targeting at a circulation region of a shopping mall in Hong Kong is presented. During Christmas days, some festival displays have been added in this area, as shown in Fig. 10. It has attracted a lot of attention from pedestrians passing by, and offers an excellent test environment for analyzing pedestrian behaviors such as 'impulse stops'.

4.1. Scenario geometry and parameter settings

The circulation region is one of the necessary ways transferring between the LG1/G/UG levels of the shopping mall and connects two important entrances. The west entrance is for pedestrians who arrive or leave the shopping mall by taxi, and the east entrance directly leads to the bus terminal. There are three visual attractors including the Christmas Display, the donating counter on northern side of the region as well as the Information map on the southern side (Fig. 11). Observations were conducted by following and eye tracking 350 pedestrians on four weekend afternoons from 2:00 to 5:00 pm in December 2013. For running the model, two entrances and two aisles are set as the main traffic generators. Data on flow rate of pedestrians at each generator, pedestrian characteristics, time for visiting attractors, and route choice between generators has been collected. To better compare the simulation results and empirical data, we also recorded a short video.

Fig. 10. Christmas Display featured as visual attractor for pedestrians passing by.

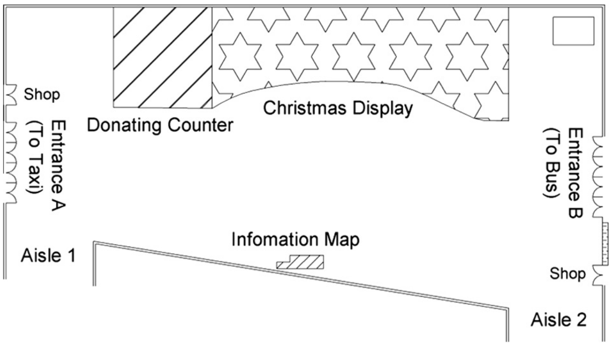

Fig. 11. Geometry of simulation scenario.

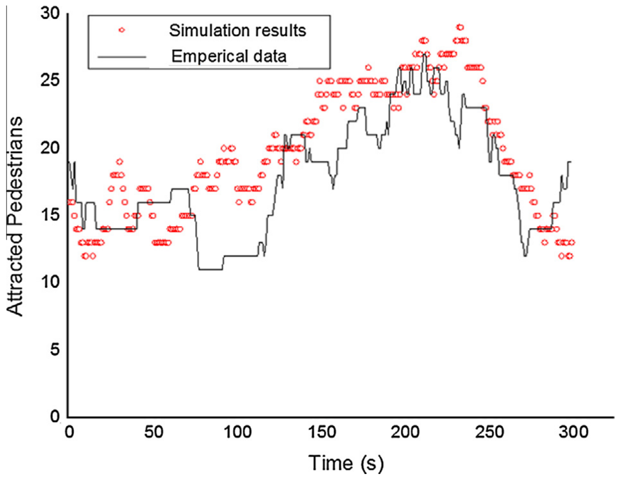

Fig. 12. Comparison of attracted pedestrians for Christmas Display between empirical data and simulation results.

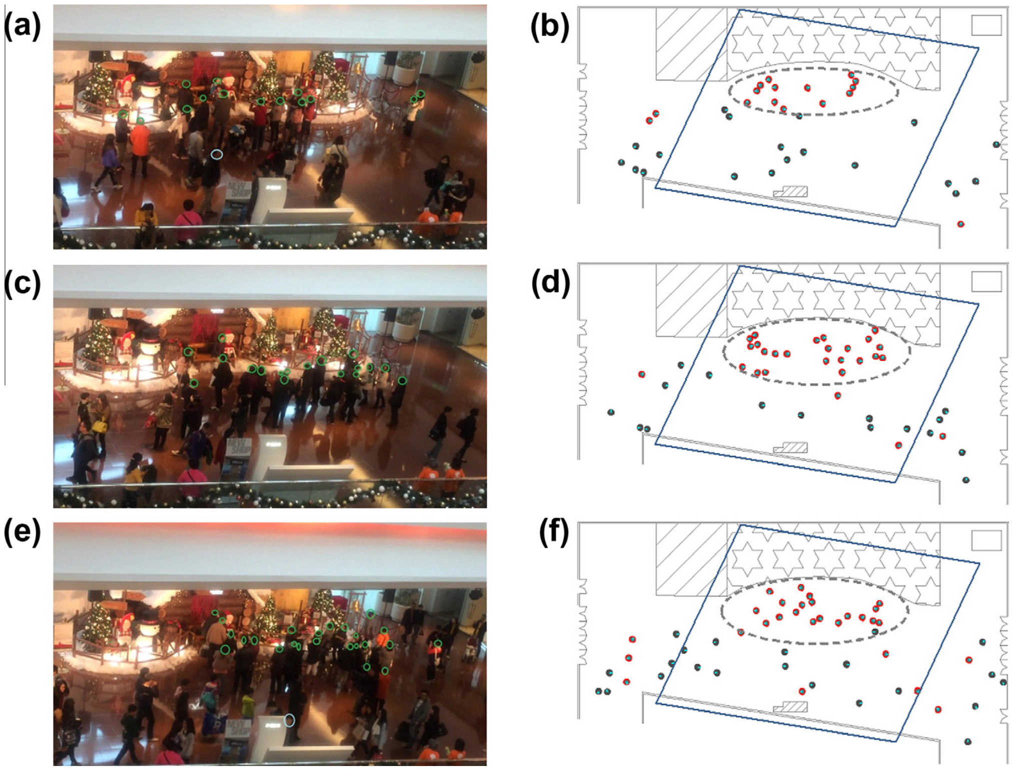

Fig. 13. Snapshot of simulation scenario: (a) Video screenshot at 25 s; (b) simulation snapshot at 25 s; (c) video screenshot at 125 s; (d) simulation snapshot at 125 s; (e) video screenshot at 225 s; (f) simulation snapshot at 225 s.

Visibility and distance weight parameters in Eq. (5) are set as follows: $\omega_v = 0.5$ and $\omega_d = 0.5$. As the scenario is part of the shopping mall, pedestrians moving inside are usually shoppers, thus we define all the pedestrians in the simulation are susceptible agents. Theoretically, the more attractive the object is, the more patronage it would have. As a result, we use the normalization values of attracted tracking numbers (pedestrians stop for the attractor) to define the attractiveness of each visual attractor in the scenario. According to tracking data, 50 pedestrians visited Christmas Display ($j = 1$), 4 visited Donating Counter ($j = 2$), and 14 visited Information map ($j = 3$). Consequently their attractiveness ratios are as follows: $\delta_1^a = 1$, $\delta_2^a = 0.08$, $\delta_3^a = 0.28$.

Despite detailed moving trajectory differences, pedestrians of same routes would possibly have similar visibility and distance conditions to the attractor during movement within the circulation region. Therefore, those pedestrians' visiting behaviors of attractors are differentiated by their internal state of demands. For example, there are 78 pedestrians traveling from Aisle 1 to Aisle 2 among our tracking records, 9 of them are attracted by Christmas Display and 3 of them are attracted by Information map. Considering the values of visibility and distance weight parameters ($\omega_v = 0.5$ and $\omega_d = 0.5$), the internal demands of this group of pedestrians are supposed to fall into three categories: 15.38% are in [0.04, 0.14), 11.54% are in [0.14, 0.5) and 73.08% are in [0.5, 1).

4.2. Results and discussions

To determine how well our model captures the attracted behavior of real pedestrians in this scenario, we compare our simulation results with empirical video data. Due to the limitation of camera shooting, this video only covers part of the scenario. Thus we record the change of attracted pedestrians in front of Christmas Display for 300 s, as shown in Fig. 12. The overall distribution of the simulation results is basically consistent with the empirical data, but it overestimates the number for certain time periods. As the time that a pedestrian stops for the attractor in simulation is assigned according to the general distribution of tracking records, which may not exactly the same with those captured in the video. As a result, longer or shorter stays of pedestrians in front of the attractor may contribute to the variances in attracted numbers.

Fig. 13(a), (c) and (e) are video screenshots of this scenario at 25 s, 125 s and 225 s, in which attracted pedestrians have been identified manually (green[1] circles represent pedestrians attracted by Christmas Display, and sky blue circles represent those attracted by Information Map). Fig. 13(b), (d) and (f) are corresponding simulation snapshots in which red circles and dark blue circles represent attracted (including both being attracted and back to scheduled route) and wandering pedestrians respectively. Area within the diamond frame corresponds to the video coverage, and pedestrians in dashed ellipse are those stopped for the attractors.

5. Conclusion

This study has presented an extended pedestrian flow simulation model—CityFlow-U by adding a new module namely the *attention-based exploratory movement module*. This module focuses on attractive interactions between pedestrians and visual attractors in the environment, in which factors of attractor's attractiveness, distance to the attractor as well as the visibility of the attractor from current location of the agent are considered in microscopic scope. Two types of agents, namely normal agent and susceptible agent are defined in this model according to their reactions to the external stimuli. And five stages of walking status have been described and related to different matching conditions of agent's internal state of demand and characteristics of external stimuli.

The parameters in the module have been analyzed by running a series of simulation tests. For the parameter ω_m, it represents the type matching result of agent's internal demand and external stimuli. Normal movement mode can be simulated by setting the value as 0, otherwise random and purposive movement modes can be revealed. Due to the physical limitations of humans, pedestrians can only perceive in certain ranges. We have shown that different attention range depths and visual angles can result in divergent attractor patronages for the same test environment. In a common shopping street setting, pedestrians tend to visit shops locating further away but more attractive when they are incorporated with a longer range depth. However, the results for different visual angles are not so obvious, as attractor alternatives do not increase a lot for pedestrians having a broader visual angle. In order to test the sensitivity of distance parameter ω_d and visibility parameter ω_v, we used different value settings to reveal interesting pedestrian movement patterns. In specific, the pedestrian movement trajectories are principally comprised of diagonal paths when visibility of the attractor (ω_v) dominates their visiting decisions. As the value of distance parameter (ω_d) increases, some of the pedestrians prefer to visit nearby shops on the same side of the street. When distance to the attractor becomes the primary concern, almost all the pedestrians refuse to visit shops across the street.

The reliability of the expanded model was also demonstrated with a simulation scenario targeting at a circulation region of a shopping mall in Hong Kong. Observations have been conducted by following and eye tracking of pedestrians, and data on flow rate of pedestrians at each generator, pedestrian characteristics, time for 'impulse stops'—visiting attractors, and route choice between generators has been collected. For comparison, the changes of attracted pedestrians in front of Christmas Display have been obtained from both simulation results and empirical video data. The overall distribution of the simulation result is basically consistent with the empirical data, but it overestimates the number for certain time periods. Because of complex human behavior, there is still a shortfall in the amount of empirical data and practical experience on more common applications. In future work, we intend to incorporate more divergent interactions between pedestrians and visual attractors, such as adding vertical attention range for pedestrians.

Acknowledgement

The work described in this paper was fully supported by a grant from the Research Grant Council, Government of the Hong Kong Administrative Region, China, No. CityU119011.

[1] For interpretation of color in Fig. 13, the reader is referred to the web version of this article.

Appendix A. Supplementary material

Supplementary data associated with this article can be found, in the online version, at http://dx.doi.org/10.1016/j.trc.2014.03.009.

References

Asano, M., Iryo, T., Kuwahara, M., 2010. Microscopic pedestrian simulation model combined with a tactical model for route choice behaviour. Transp. Res. Part C: Emerg. Technol. 18 (6), 842–855.

Bandini, S., Federici, M.L., Vizzari, G., 2007. Situated cellular agents approach to crowd modeling and simulation. Cybern. Syst. 38 (7), 729–753.

Bandini, S., Rubagotti, F., Vizzari, G., Shimura, K., 2011. An agent model of pedestrian and group dynamics: experiments on group cohesion. In: Pirrone, R., Sorbello, F. (Eds.), AI*IA 2011: Artificial Intelligence Around Man and Beyond. Springer, Berlin, Heidelberg, pp. 104–116.

Bandini, S., Mondini, M., Vizzari, G., 2014. Modelling negative interactions among pedestrians in high density situations. Transp. Res. Part C: Emerg. Technol. 40, 251–270.

Borgers, A., Timmermans, H., 1986. A model of pedestrian route choice and demand for retail facilities within inner-city shopping areas. Geogr. Anal. 18 (2), 115–128.

Burstedde, C., Klauck, K., Schadschneider, A., Zittartz, J., 2001. Simulation of pedestrian dynamics using a two-dimensional Cellular Automaton. Physica A 295 (3–4), 507–525.

Chen, C.H., 2011. Attention theory-based agent system: using shopping street design simulation as an example. J. Chin. Inst. Eng. 34 (1), 155–168.

Cobb, C.J., Hoyer, W.D., 1986. Planned versus impulse purchase behavior. J. Retail. 62, 384–409.

Dai, J.c., Li, X., Liu, L., 2013. Simulation of pedestrian counter flow through bottlenecks by using an agent-based model. Physica A 392 (9), 2202–2211.

Davidich, M., Geiss, F., Mayer, H.G., Pfaffinger, A., Royer, C., 2013. Waiting zones for realistic modelling of pedestrian dynamics: a case study using two major German railway stations as examples. Transp. Res. Part C: Emerg. Technol. 37, 210–222.

Dijkstra, J., 2008. An agent architecture for visualizing simulated human behavior to support the assessment of design performance. In: 2008 International Conference on Computational Intelligence for Modelling Control & Automation, pp. 808–813.

Dijkstra, J., Jessurun, J., Timmermans, H., de Vries, B., 2011. A framework for processing agent-based pedestrian activity simulations in shopping environments. Cybern. Syst. 42 (7), 526–545.

Gibson, E.J., 1988. Exploratory behavior in the development of perceiving, acting, and the acquiring of knowledge. Annu. Rev. Psychol. 39 (1), 1–42.

Guo, R.Y., Wong, S.C., Huang, H.J., Zhang, P., Lam, W.H.K., 2010. A microscopic pedestrian-simulation model and its application to intersecting flows. Physica A 389 (3), 515–526.

Helbing, D., Molnár, P., 1995. Social force model for pedestrian dynamics. Phys. Rev. E 51 (5), 4282–4286.

Hua, K., Xing-Li, L., Yan-Fang, W., Tao, S., Shi-Qiang, D., 2010. Effect of following strength on pedestrian counter flow. Chin. Phys. B 19 (7), 070517.

Kwak, J., Jo, H.-H., Luttinen, T., Kosonen, I., 2013. Collective dynamics of pedestrians interacting with attractions. Phys. Rev. E 88 (6), 062810.

Liu, S.B., Lo, S.M., Ma, J., Wang, W.L., 2014. An agent-based microscopic pedestrian flow simulation model for pedestrian traffic problems. IEEE Trans. Intell. Transp. Syst. (in press), http://dx.doi.org/10.1109/TITS.2013.2292526.

Lo, S.M., Fang, Z., Lin, P., Zhi, G.S., 2004. An evacuation model: the SGEM package. Fire Saf. J. 39 (3), 169–190.

Ma, J., Song, W.G., Zhang, J., Lo, S.M., Liao, G.X., 2010. K-Nearest-Neighbor interaction induced self-organized pedestrian counter flow. Physica A 389 (10), 2101–2117.

Ma, J., Lo, S.M., Song, W.G., Wang, W.L., Zhang, J., Liao, G.X., 2013. Modeling pedestrian space in complex building for efficient pedestrian traffic simulation. Automat. Constr. 30, 25–36.

Moussaïd, M., Helbing, D., Theraulaz, G., 2011. How simple rules determine pedestrian behavior and crowd disasters. Proc. Natl. Acad. Sci. 108 (17), 6884–6888.

Nassar, K., 2011. Sign visibility for pedestrians assessed with agent-based simulation. Transp. Res. Re.: J. Transp. Res. Board 2264 (1), 18–26.

Park, J.H., Rojas, F.A., Yang, H.S., 2013. A collision avoidance behavior model for crowd simulation based on psychological findings. Comput. Animat. Virtual Worlds 24 (3–4), 173–183.

Schelhorn, T., O'Sullivan, D., Haklay, M., Thurstain-Goodwin, M., 1999. STREETS: An Agent-based Pedestrian Model. Presented at Computers in Urban Planning and Urban Management, Venice, 8–11 September. <http://www.casa.ucl.ac.uk/~david/AnAgent.pdf>.

Shiwakoti, N., Sarvi, M., 2013. Enhancing the panic escape of crowd through architectural design. Transp. Res. Part C: Emerg. Technol. 37, 260–267.

Song, X., Duh, H.B.L., 2010. A simulation of bonding effects and their impacts on pedestrian dynamics. IEEE Trans. Intell. Transp. Syst. 11 (1), 153–161.

Timmermans, H.J., 2009. Impulse and Non-Impulse Store Choice Processes in a Multi-Agent Simulation of Pedestrian Activity in Shopping Environments, Pedestrian Behavior: Models, Data Collection and Applications. Emerald Group Publishing, pp. 63–85.

Turner, A., Penn, A., 2002. Encoding natural movement as an agent-based system: an investigation into human pedestrian behaviour in the built environment. Environ. Plan. B: Plan. Des. 29 (4), 473–490.

Turner, A., Doxa, M., O'Sullivan, D., Penn, A., 2001. From isovists to visibility graphs: a methodology for the analysis of architectural space. Environ. Plan. B: Plan. Des. 28 (1), 103–121.

Xi, H., Lee, S., Son, Y.-J., 2011. An integrated pedestrian behavior model based on extended decision field theory and social force model. In: Rothrock, L., Narayanan, S. (Eds.), Human-in-the-Loop Simulations. Springer, London, pp. 69–95.

Yin, L., 2013. Assessing walkability in the city of buffalo: application of agent-based simulation. J. Urban Plan. Dev. 139 (3), 166–175.

Yuen, J.K.K., Lee, E.W.M., Lo, S.M., Yuen, R.K.K., 2013. An intelligence-based optimization model of passenger flow in a transportation station. IEEE Trans. Intell. Transp. Syst. 14 (3), 1290–1300.

Zacharias, J., 1997. The impact of layout and visual stimuli on the itineraries and perceptions of pedestrians in a public market. Environ. Plan. B: Plan. Des. 24, 23–36.

Zacharias, J., 2001. Pedestrian behavior pedestrian behavior and perception in urban walking environments. J. Plan. Literature 16 (1), 3–18.

Zeng, W., Chen, P., Nakamura, H., Iryo-Asano, M., 2014. Application of social force model to pedestrian behavior analysis at signalized crosswalk. Transp. Res. Part C: Emerg. Technol. 40, 143–159.

Zheng, X., Zhong, T., Liu, M., 2009. Modeling crowd evacuation of a building based on seven methodological approaches. Build. Environ.: Plan. Des. 44 (3), 437–445.

Zhuang, G., Tsang, A.S., Zhou, N., Li, F., Nicholls, J., 2006. Impacts of situational factors on buying decisions in shopping malls: an empirical study with multinational data. Eur. J. Mark. 40 (1/2), 17–43.